Cooperative Adaptive Cruise Control for String Stable Mixed Traffic: Benchmark and Human-Centered Design

Fangjian Li, *Student Member, IEEE*, and Yue Wang, *Senior Member, IEEE*

***Abstract*— With the emergence of vehicle-to-vehicle communication technology, cooperative adaptive cruise control (CACC) cars can be expected in the near future. In this paper, novel criteria for string stability are proposed for mixed traffic platoons that consist of both automated and manual driving cars. A mixed traffic string stability definition is proposed to guarantee the boundedness of the motion states fluctuation upstream as well as the safety of the entire platoon. With proper arrangements of the platoon sequence as well as mild restrictions on the leading car's velocity overshoot, the proposed mixed traffic string stability can be realized via some suitable controller design for the automated cars. The benchmark controller with feedback and feedforward path is first used to verify the above results with rigorous proof. Furthermore, a human-centered CACC system is designed to improve both physical and psychological comfort of a driver under the guarantee of mixed traffic string stability. The action-point car-following model is adapted to quantify the driver's psychological comfort in combination with the quantification of physical comfort based on jerk. A model predictive control-like blending ratio controller is developed to obtain the optimal time headway in the feedback controller for tradeoffs among driver comfort, fuel efficiency, and traffic throughput under string stability constraints. Finally, a seven-car CACC mixed traffic platoon scenario is simulated. Compared with the benchmark CACC controller design, the human-centered CACC design is shown to largely improve the driving comfort.**

***Index Terms*— Cooperative adaptive cruise control (CACC), mixed traffic, string stability, human-centered controller.**

I. Introduction

CURRENTLY, adaptive cruise control (ACC) systems can be equipped in almost every newly-launched car and is proved to outperform common human drivers [1]. More recently, thanks to the vehicle-to-vehicle (V2V) communication technology, the cooperative adaptive cruise control (CACC) system is proposed [2]. Compared to ACC, CACC is expected to result in a much shorter headway and hence a better performance in terms of throughput, fuel consumption and emission [3]. However, the adoption of exclusively automated cruise control cars in real traffic is still unrealistic in the near future. As a result, the research on mixed traffic platoon, in which automated cars and manual driving cars share a same traffic lane, is of great importance.

In the literature, there are many different definitions for the stability of a car platoon. Early works regard the platoon as an interconnected system and analyze its Lyapunov stability. In [4], it is proposed that Lyapunov stability can be satisfied when the motion states of the platoon are always bounded under some initial condition perturbations. In [5], the least stable eigenvalue of the platoon system matrix is used as a measure of stability margin. However, the mere boundedness of motion states under initial condition perturbations cannot guarantee a well-behaved platoon because the large state fluctuation brought by the change of leading car's velocity profile can still cause problems from the traffic and safety aspects, such as congestion [6] and collision [7].

Therefore, the platoon behavior under a varying velocity profile of the leading car needs to be investigated. The definition of string stability has been widely adopted, which requires that the motion fluctuation caused by external inputs from the leading car should not propagate upstream [8]. Nevertheless, there is so far no unified conclusion about how to measure and quantify the platoon fluctuation. In [9], the spacing error between the actual and desired inter-vehicle distance is chosen as the measurement of platoon fluctuation. String stability is satisfied if the 2-norm of the spacing error does not propagate upstream. Based on the input-output theory for linear systems [10], this is equivalent to having H_∞ norm of the transfer function of the spacing error of two adjacent cars to be less than or equal to one.

In [11], a relaxed criterion for the mixed traffic platoon scenario is proposed, which only requires the transfer function of the spacing error from the first following car to the last following car to be no larger than 1. In [12], it is found that motion states (i.e. velocity and acceleration), compared to the spacing error, should be a better choice for heterogeneous platoons since their corresponding transfer functions do not depend on other cars' dynamics.

More generally, in [13], the platoon fluctuation is quantified by the p-norm of the fluctation measurements, where p can be any integer from 1 to ∞. From the input-output theory of linear systems, the 1-norm of the inverse Laplace transform of the above error transfer functions should always be less than or equal to 1 to guarantee string stability when the

Manuscript received November 27, 2016; revised May 11, 2017 and September 20, 2017; accepted October 3, 2017. Date of publication November 3, 2017; date of current version December 7, 2017. The Associate Editor for this paper was F. Lian. *(Corresponding author: Yue Wang.)*

The authors are with the Department of Mechanical Engineering, Clemson University, Clemson, SC 29634 USA (e-mail: yue6@clemson.edu; fangjil@clemson.edu).

Color versions of one or more of the figures in this paper are available online at http://ieeexplore.ieee.org.

Digital Object Identifier 10.1109/TITS.2017.2760805

fluctuation is quantified by the ∞-norm. A similar criterion is proposed in [14], which requires the p norm of the output signal should be bounded by the class $\mathcal{K}$ functions of the p norm of the input of the leading car and the initial states deviation from the equilibrium. Compared to the conventional feedback and feedforward controller design to guarantee H_∞ string stability, larger time headway and controller gain are adopted therein.

Although the above H_∞ and $\mathcal{L}_p$ string stability definitions can be applied for heterogeneous CACC platoons, the resulting transfer function of consecutive cars fails to serve as a criterion for stability analysis in mixed traffic due to the presence of manual cars. Due to human limits such as long reaction time and low sensitivity to velocity changes, a manual driving car can easily break the above conventional string stability conditions [13]. Therefore, a more general string stability definition for mixed traffic platoons is necessary.

The CACC system belongs to Level 1 Automation with a human-in-the-loop according to the definition given by the national highway traffic safety admistration (NHTSA) [15]. Therefore, the interaction between a human driver and the CACC system is inevitable and critical to the joint operation system. In general, we can categorize human factors in CACC controller design into two aspects: physical and psychological comfort. Physical comfort is directly related to the receptors of the human, such as motion sickness. Psychological comfort is related to human's cognition and emotion [16].

Although there is a lot of research in cruise control design taking into account driver's physical comfort [17]–[19], the automated controller considering psychological comfort has not been well addressed. In [20], the large spacing error deviation is regarded as unnatural to the driver, which may cause psychological discomfort. The cruise control is designed to minimize the spacing error transfer function magnitude from the preceding car's velocity to that of the current car. In [21], it is proposed that driving at an unacceptably close distance to the preceding car is impolite. As a result, a minimum limit for the desired headway should be adopted even though safety can be guaranteed. In this paper, a human-centered CACC controller design is proposed to improve the psychological comfort of the cruise control besides the phyiscal comfort aspect considered by Wang and Wang [18]. Here, we consider that the CACC controller improves human's psychological comfort if the human driver is less disrupted by the rapid interaction with the preceding car. The concept of unconscious regime in the action-point (AP) car-following model [22] is adopted to minimize the human driver's perception of motion changes of the preceding car. In addition, a minimum distance headway is set to obey the social rules.

In summary, the main contribution of the paper is two-fold: Firstly, a novel definition for mixed traffic string stability is proposed, which can guarantee both an acceptable platoon behavior and the platoon safety. To the best of the authors' knowledge, very few works have considered a formal quantititive defintion of string stability in mixed traffic platoons [11]. The mixed traffic string stability with the benchmark linear controller is verified analytically and demonstrated numerically. Secondly, a human-centered controller taking into account both physical and psychological comfort is developed. A model predictive control (MPC)-like blending ratio controller is developed to realize reasonable trade-offs among driver physical comfort, psychological comfort, traffic efficiency and fuel economy while guaranteeing mixed traffic string stability.

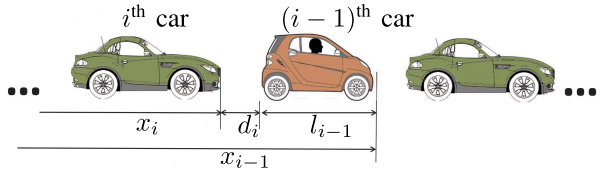

Fig. 1. Illustration of the mixed traffic platoon.

The rest of the paper is organized as follows. In Section II, the mixed traffic platoon scenario is defined. In addition, the reason why the conventional string stability criteria for automated platoon is not suitable for mixed traffic is discussed. In Section III, a novel definition of the mixed traffic string stability is proposed. The conditions for the platoon to satisfy the defined mixed traffic string stability are generated. In Section IV, the structure of the benchmark CACC controller as well as the whole platoon model are formulated. The proof of mixed traffic string stability under the benchmark control structure is also provided. In Section V, a human-centered controller is developed to enhance the driver experience in using CACC. In Section VI, mixed traffic platoon with both benchmark and human-centered CACC controller designs are simulated and compared. Section VII provides the summary, conclusion, and future works.

II. Problem Setup

A. Mixed Traffic Scenario

Definition 1 (Mixed Traffic Platoon): The mixed traffic platoon is a string of automated (ACC and/or CACC) and manual driving cars driving along a same lane with short inter-distances. The leading car's time-varying velocity profile is taken as the external input of the mixed traffic platoon, which is also the major source of velocity perturbation of the platoon. Each following car only executes the car-following task based on its preceding cars' motion states or inter-distance. The leading car can be either a manual driving or an automated car operated under the guidance of traffic infrastructures. The sequence of following cars can be arbitrary.

Based on the parameters shown in Fig. 1, several types of transfer functions will be introduced as follows. Since the car length is fixed and can be subtracted from distance calculation, a car is considered as a point mass without length ($l_i = 0$) for simplicity. Firstly, denote $\lambda_i(t) \in \{a_i(t), v_i(t)\}$ as the motion states where $a_i(t)$ and $v_i(t)$ are the acceleration and velocity of the i^{th} car, respectively. Let the index of the leading car be 1. Define the motion states transfer function from the j^{th} car to the i^{th} car as follows:

$$G^{\Lambda}_{i,j}(s) \triangleq \frac{\Lambda_i(s)}{\Lambda_j(s)}, \quad i \geq j \geq 1. \tag{1}$$

where $\Lambda_i(s)$ ($\Lambda_j(s)$) is the Laplace transform of $\lambda_i(t)$ ($\lambda_j(t)$). In addition, we use $\Phi(i) \in \{H, A, C\}$ to denote the type of the i^{th} car, where H, A and C represent the sets of the manual driving, ACC, and CACC cars, respectively.

If the predecessor-following (PF) information flow topology [2] is adopted, i.e. only the information of the immediate preceding car is taken into account, we define $G^*_{\Phi(i)}$ as the motion states transfer function from any type of preceding car to the immediate following car with type $\Phi(i)$. That is,

$$G^*_{\Phi(i)} \triangleq G^{\Lambda}_{i,i-1}(s), \quad i > 1. \tag{2}$$

Denote the inter-distance between the i^{th} and $i-1^{\text{th}}$ car as $d_i(t)$, i.e. $d_i = x_{i-1}(t) - x_i(t)$, $i > 1$. Define the inter-distance transfer function from the j^{th} car to the i^{th} car as

$$G^D_{i,j}(s) \triangleq \frac{D_i(s)}{D_j(s)}, \quad i \geq j > 1,$$

where $D_i(s)(D_j(s))$ is Laplace transform of $d_i(t)(d_j(t))$. Specially, for two adjacent cars, we have:

$$\begin{aligned} G^D_{i,i-1}(s) &= \frac{D_i(s)}{D_{i-1}(s)} = \frac{X_i(s) - X_{i-1}(s)}{X_{i-1}(s) - X_{i-2}(s)} \\ &= \frac{\frac{1}{s}V_{i-1}(s) - \frac{1}{s}V_i(s)}{\frac{1}{s}V_{i-2}(s) - \frac{1}{s}V_{i-1}(s)} \\ &= \frac{1 - G^{\Lambda}_{i,i-1}(s)}{1 - G^{\Lambda}_{i-1,i-2}(s)} G^{\Lambda}_{i-1,i-2}(s), \quad i > 2. \end{aligned} \tag{3}$$

B. Automated Platoon String Stability

Various criteria of string stability for either homogeneous or heterogeneous automated platoons have been proposed in the literature. These criteria require the following car's fluctuation should not be larger than that of the preceding car. However, the quantification and measurement of the fluctuation are different. For example, [11] and [12] use the 2 norm to quantify the fluctuation, while [14] and [13] consider the infinity norm. For the measurements of string stability, velocity and spacing error are the most common choices. In addition, both the 2 norm and infinity norm criteria have their sufficient conditions represented by transfer function.

For the 2 norm criterion, because $\|\mathcal{L}^{-1}(G(s)U(s))\|_2 \leq \|G(s)\|_{H_\infty}\|\mathcal{L}^{-1}(U(s))\|_2$ based on input-output theorem [10] with input $U(s)$ and output $G(s)U(s)$, assuming that the platoon reaches the equilibrium λ^e when $\lambda_i(0) = \lambda_1(0) = \lambda^e, \forall i > 1$, the general expression for string stability is:

$$\frac{\|\lambda_i(t) - \lambda_i(0)\|_2}{\|\lambda_{i-1}(t) - \lambda_{i-1}(0)\|_2} \leq \|G^{\Lambda}_{i,i-1}(s)\|_{H_\infty} \leq 1, \quad \forall i > 1,\ t > 0. \tag{4}$$

For the infinity norm criterion, because $\|\mathcal{L}^{-1}(G(s)U(s))\|_\infty \leq \|\mathcal{L}^{-1}(G(s))\|_1\|\mathcal{L}^{-1}(U(s))\|_\infty$ [10], the general expression for string stability is

$$\frac{\|\lambda_i(t) - \lambda_i(0)\|_\infty}{\|\lambda_{i-1}(t) - \lambda_{i-1}(0)\|_\infty} \leq \|g^{\Lambda}_{i,i-1}(t)\|_1 \leq 1, \quad \forall i > 1,\ t > 0, \tag{5}$$

where $g^{\Lambda}_{i,i-1}(t) = \mathcal{L}^{-1}(G^{\Lambda}_{i,i-1}(s))$ and λ_i is the measurement of fluctuation in terms of motion states. The expressions are similar when the fluctuation is measured by the spacing error.

Remark 1: The criteria in inequalities (4) and (5) for automated platoons concentrate on the relation between the following car and its immediate preceding car. However, numerous research, such as [13], has shown that the human drivers behave an accordion effect that will propagate the motion states oscillation. Hence, (4) and (5) cannot be satisfied mathematically. As a result, the string stability criteria for automated platoons are not applicable to the mixed traffic platoons if manual driving cars are involved. •

To address this issue, in the next section, a novel definition for mixed traffic string stability will be proposed.

III. String Stability for Mixed Traffic Platoon

Traffic congestion is a severe problem in transportation and the propagation of velocity fluctuation upstream is a leading factor [23]. It is hence reasonable to propose a definition of string stability corresponding to the suppression of this effect. As a result, the mixed traffic string stability should guarantee an acceptable fluctuation upstream caused by the time-variant velocity profile of the leading car. In addition, the rear-end collision should be avoided to guarantee safety. Based on the above requirements, we have the following definition.

Definition 2 (Mixed Traffic String Stability): For the mixed traffic platoon defined in Definition 1, assuming that the platoon reaches the equilibrium when $\lambda_i(0) = \lambda_1(0) = \lambda^e$, $\forall i > 1$, the platoon is string stable if:

$$\|\lambda_i(t) - \lambda_i(0)\|_2 \leq \|G^*_{h_a}(s)\|_{H_\infty}\|\lambda_1(t) - \lambda_1(0)\|_2, \quad i > 1. \tag{6}$$

$$\|\lambda_i(t) - \lambda_i(0)\|_\infty \leq \|g^*_{h_a}(t)\|_1\|\lambda_1(t) - \lambda_1(0)\|_\infty, \quad i > 1. \tag{7}$$

$$x_i(t) < x_{i-1}(t), \quad \forall t > 0, \quad i > 1. \tag{8}$$

where $h_a \in H$ is a standard type of manual driving car, which is used as a reference for the platoon's behavior and $g^*_{h_a}(t) = \mathcal{L}^{-1}(G^*_{h_a}(s))$.

Remark 2: Different car-following models can be adopted as standard manual driving car. For example, we can use the Pipe model in which the acceleration of the following car depends on the velocity difference with the preceding car, human's reaction delay, sensitivity factor and the mass of the car [24]. According to the average value calibrated by [24], it follows that $\|G^*_{h_a}(s)\|_\infty = 1.03 > 1$ and $\|g^*_{h_a}(t)\|_1 = 1.328 > 1$. •

Remark 3: The inequalities (6) and (7) give the relation between the motion states fluctuation of every following car ($\lambda_i(t) - \lambda_i(0)$) and that of the leading car ($\lambda_1(t) - \lambda_1(0)$). From the input-output theorem [10], if the second car is a manual driving car, we also have $\|\lambda_2(t) - \lambda_2(0)\|_2 \leq \|G^*_{h_a}(s)\|_{H_\infty}\|\lambda_1(t) - \lambda_1(0)\|_2$ and $\|\lambda_2(t) - \lambda_2(0)\|_\infty \leq \|g^*_{h_a}(t)\|_1\|\lambda_1(t) - \lambda_1(0)\|_\infty$. The above two inequalities share the same right hand side with (6) and (7). It is required that the motion fluctuation in every following car is bounded by the fluctuation when the standard manual driving car directly follows the leading car. When the 2 norm is adopted in (6), the fluctuation in the platoon is quantified from the energy

aspect. When the ∞ norm is adopted in (7), the fluctuation is quantified by the maximum overshoot. •

Remark 4: The mere boundedness of motion states is not enough to guarantee safety of the whole platoon. Therefore, the inequality (8) is necessary to restrict the position of any following car not to exceed that of its preceding car. •

Remark 5: This paper only focuses on the scenario that is initiated from the equilibrium which can be regarded as the platoon maintaining problem that has attracted many research interests [6]. The initiation from equilibrium is reasonable since the main task of a platoon in highway is cruising under constant velocity [25]. •

The following theorem is proposed to check the mixed traffic string stability.

Theorem 1: Consider the mixed traffic platoon defined in Definition 1. Let the leading car's velocity profile be v_1. Assume that the automated cars adopt the constant time headway (CTH) policy [13] and all the cars adopt the predecessor-following (PF) information topology [2]. The system is mixed traffic string stable according to Definition 2 if:

$$\|G^{\Lambda}_{i,1}(s)\|_{H_\infty} \le \|G^{*}_{h_a}(s)\|_{H_\infty},\ \forall\, i > 1, \tag{9}$$

$$\|g^{\Lambda}_{i,1}(t)\|_1 \le \|g^{*}_{h_a}(t)\|_1,\ \forall\, i > 1, \tag{10}$$

$$\|v_1(t) - v_1(0)\|_\infty \le \min\left(\frac{h_{\Phi(i)}v_1(0)}{\|g'_{\Phi(i)}(t)\|_1\|g^{*}_{h_a}(t)\|_1},\ \frac{h_{\Phi(2)}v_1(0)}{\|g'_{\Phi(2)}(t)\|_1}\right),\quad \forall i > 2, \tag{11}$$

where $h_{\Phi(i)}$ is the constant time headway for the cars with type $\Phi(i)$, $G'_{\Phi(i)}(s) \triangleq (1-G^{*}_{\Phi(i)}(s))\frac{1}{s}$ and $g'_{\Phi(i)} \triangleq \mathcal{L}^{-1}(G'_{\Phi(i)}(s))$.

Proof: From [10], based on (1) and (9), we have:

$$\begin{aligned}\|\lambda_i(t) - \lambda_i(0)\|_2 &\le \|G^{\Lambda}_{i,1}(s)\|_{H_\infty}\|\lambda_1(t) - \lambda_1(0)\|_2\\ &\le \|G^{*}_{h_a}(s)\|_{H_\infty}\|\lambda_1(t) - \lambda_1(0)\|_2.\end{aligned}$$

As a result, the inequality (6) is satisfied. Similarly, based on the input-output characteristics and (10), we have:

$$\begin{aligned}\|\lambda_i(t) - \lambda_i(0)\|_\infty &\le \|g^{\Lambda}_{i,1}(t)\|_1\|\lambda_1(t) - \lambda_1(0)\|_\infty\\ &\le \|g^{*}_{h_a}(t)\|_1\|\lambda_1(t) - \lambda_1(0)\|_\infty.\end{aligned}$$

As a result, the inequality (7) is satisfied. The proof of condition (8) is as follows. From (2) and (3), we have:

$$\begin{aligned}G^{D}_{i,2}(s) &= \frac{1-G^{\Lambda}_{i,i-1}(s)}{1-G^{\Lambda}_{2,1}(s)}G^{\Lambda}_{i-1,1}(s),\\ &= \frac{1-G^{*}_{\Phi(i)}(s)}{1-G^{*}_{\Phi(2)}(s)}G^{\Lambda}_{i-1,1}(s),\quad i > 2.\end{aligned} \tag{12}$$

In addition, we can also get $D_2(s) = (V_1(s) - V_2(s))\frac{1}{s} = V_1(s)\left(1 - G^{*}_{\Phi(2)}(s)\right)\frac{1}{s}$ and hence $\frac{D_2(s)}{V_1(s)} = \left(1 - G^{*}_{\Phi(2)}(s)\right)\frac{1}{s}$. Therefore, we can obtain the follows:

$$\begin{aligned}G_{D_i,V_1}(s) &= \frac{D_i(s)}{V_1(s)} = \frac{D_i(s)}{D_2(s)}\frac{D_2(s)}{V_1(s)}\\ &= \frac{1-G^{*}_{\Phi(i)}(s)}{1-G^{*}_{\Phi(2)}(s)}\left(1 - G^{*}_{\Phi(2)}(s)\right)\frac{1}{s}G^{\Lambda}_{i-1,1}(s)\\ &= \left(1 - G^{*}_{\Phi(i)}(s)\right)\frac{1}{s}G^{\Lambda}_{i-1,1}(s)\\ &= G'_{\Phi(i)}(s)G^{\Lambda}_{i-1,1}(s),\quad i > 2.\end{aligned}$$

Based on the Young's Inequality [26] and (10), we have the following about the 1-norm of inverse Laplace transform:

$$\begin{aligned}\|g_{D_i,V_1}(t)\|_1 &\le \|g'_{\Phi(i)}(t)\|_1\|g^{\Lambda}_{i-1,1}(t)\|_1\\ &\le \|g'_{\Phi(i)}(t)\|_1\|g^{*}_{h_a}(t)\|_1,\quad i > 2.\end{aligned}$$

Since $D_i(s) = G_{D_i,V_1}(s)V_1(s),\ i > 2$, based on the linear input-output system property [10], we have,

$$\begin{aligned}\|d_i(t) - d_i(0)\|_\infty &\le \|g_{D_i,V_1}(t)\|_1\|v_1(t) - v_1(0)\|_\infty\\ &\le \|g'_{\Phi(i)}(t)\|_1\|g^{*}_{h_a}(t)\|_1\|v_1(t) - v_1(0)\|_\infty,\quad i > 2.\end{aligned} \tag{13}$$

Substituting (11) into (13), we have $\|d_i(t) - d_i(0)\|_\infty \le h_{\Phi(i)}v_1(0),\ i > 2$. Since we assume that the platoon reaches its equilibrium at $t = 0$ in Definition 2, at the beginning, every car should be at the same velocity and the inter-distance should equal to its desired headway, i.e. $v_i(0) = v_1(0) = v^e$, $d_i(0) = v_i(0)h_{\Phi(i)}, \forall i \ge 2$. As a result, (13) becomes

$$\|d_i(t) - d_i(0)\|_\infty \le h_{\Phi(i)}v_1(0) = d_i(0),\quad \forall i > 2. \tag{14}$$

As can be seen from (14), $d_i(t) > 0,\quad \forall i > 2$. Similarly, for $i = 2$, we have $D_2(s) = G'_{\Phi(2)}(s)V_1(s)$ and

$$\|d_2(t) - d_2(0)\|_\infty \le \|g'_{\Phi(2)}(t)\|_1\|v_1(t) - v_1(0)\|_\infty \tag{15}$$

Substituting the inequality (11) into (15), it follows that $\|d_2(t) - d_2(0)\|_\infty \le h_{\Phi(2)}v_1(0) = d_2(0)$. Therefore, we have $d_2(t) > 0$. Finally, combined with (14), the safety condition (8) is guaranteed ($d_i(t) > 0, \forall i \ge 2$). ■

Remark 6: From Theorem 1, we can conclude that the suitable design of the automated systems, the arrangement of the mixed traffic sequence, i.e. the inequalities (9), (10) and the restriction on the leading car's velocity overshoot (11) will together guarantee the mixed traffic string stability. •

The inequalities (9) and (10) require to get the exact value or upper bound of the norms for every car in the platoon, which might become a burden if the platoon is too long. We next discuss how to simplify this process.

Proposition 1: For Theorem 1, assume $\|G^{*}_{h_a}\|_{H_\infty} \ge 1$ and $\|g^{*}_{h_a}(t)\|_1 \ge 1$, if the automated cars are designed such that:

$$\|G^{*}_{\Phi(i)}(s)\|_{H_\infty} \le 1,\quad \forall\Phi(i) \in A \cup C. \tag{16}$$

$$\|g^{*}_{\Phi(i)}(t)\|_1 \le 1,\quad \forall\Phi(i) \in A \cup C. \tag{17}$$

the inequalities (9), (10) and (11) can be changed into the following inequalities $\forall\ i > 1$:

$$\|G^{\Lambda}_{i,1}(s)\|_{H_\infty} \le \|G^{*}_{h_a}(s)\|_{H_\infty}, \forall\Phi(i) \in H, \tag{18}$$

$$\|g^{\Lambda}_{i,1}(t)\|_1 \le \|g^{*}_{h_a}(t)\|_1, \forall\Phi(i) \in H, \tag{19}$$

$$\|v_1(t) - v_1(0)\|_\infty \le \min\left(\frac{h_{\Phi(i)}v_1(0)}{\|g'_{\Phi(i)}(t)\|_1\|g^{*}_{h_a}(t)\|_1}\right) \tag{20}$$

Proof: Let the indexes of manual-driving cars in the platoon be $k_1, k_2, k_3, \ldots, k_n$ where $k_1 < k_2 < \ldots < k_n$. With the sub-multiplicative property of transfer function, we can get the following inequalities to show the satisfaction of (9).

For the automated cars in front the first manual driving car k_1, under the assumption (16), we have:

$$\begin{aligned}\|G^{\Lambda}_{i,1}(s)\|_{H_\infty} &\leq \prod_{j=2}^{i} \|G^{*}_{\Phi(j)}(s)\|_{H_\infty} \leq 1 \\ &\leq \|G^{*}_{h_a}(s)\|_{H_\infty}, \quad \forall i < k_1 \end{aligned} \tag{21}$$

For a manual driving car, directly from (18), we have:

$$\|G^{\Lambda}_{i,1}(s)\|_{H_\infty} \leq \|G^{*}_{h_a}(s)\|_{H_\infty}, \quad \forall i \in \{k_1, k_2, \ldots, k_n\} \tag{22}$$

For the automated cars between manual driving cars or after the last manual driving car, from (16) and (18), we have

$$\begin{aligned}\|G^{\Lambda}_{i,1}(s)\|_{H_\infty} &\leq \prod_{j=k_m+1}^{i} \|G^{*}_{\Phi(j)}(s)\|_{H_\infty} \|G^{\Lambda}_{k_m,1}(s)\|_{H_\infty} \\ &\leq \|G^{*}_{h_a}(s)\|_{H_\infty} \\ &\quad \forall k_m < i < k_{m+1}, \\ 1 \leq m < n, \text{ or } k_m < i, \ m = n \end{aligned} \tag{23}$$

Hence, based on (21)-(23), the inequality (9) is satisfied. For (10), with Young's Inequality, we have the following proof:

$$\begin{aligned}&\|g^{\Lambda}_{i,1}(s)\|_1 \leq \prod_{j=2}^{i} \|g^{*}_{\Phi(j)}(s)\|_1 \leq 1 \leq \|g^{*}_{h_a}(s)\|_1, \quad \forall i < k_1, \\ &\|g^{\Lambda}_{i,1}(s)\|_1 \leq \|g^{*}_{h_a}(s)\|_1, \ \forall i \in \{k_1, k_2, \ldots, k_n\} \\ &\|g^{\Lambda}_{i,1}(s)\|_1 \leq \prod_{j=k_m+1}^{i} \|g^{*}_{\Phi(j)}(s)\|_1 \|g^{\Lambda}_{k_m,1}(s)\|_1 \leq \|g^{*}_{h_a}(s)\|_1, \\ &\qquad \forall k_m < i < k_{m+1}, \quad 1 \leq m < n, \quad \text{or } i > k_m, \quad m = n. \end{aligned}$$

For the condition (11), since $\|g^{*}_{h_a}(t)\|_1 \geq 1$, we have $\frac{h_{\Phi(2)} v_1(0)}{\|g'_{\Phi(2)}(t)\|_1 \|g^{*}_{h_a}(t)\|_1} \leq \frac{h_{\Phi(2)} v_1(0)}{\|g'_{\Phi(2)}(t)\|_1}$. As a result, $\forall i > 1$

$$\begin{aligned}&\min\left(\frac{h_{\Phi(i)} v_1(0)}{\|g'_{\Phi(i)}(t)\|_1 \|g^{*}_{h_a}(t)\|_1}\right) \\ &= \min\left(\frac{h_{\Phi(j)} v_1(0)}{\|g'_{\Phi(j)}(t)\|_1 \|g^{*}_{h_a}(t)\|_1}, \frac{h_{\Phi(2)} v_1(0)}{\|g'_{\Phi(2)}(t)\|_1 \|g^{*}_{h_a}(t)\|_1}\right) \\ &\leq \min\left(\frac{h_{\Phi(j)} v_1(0)}{\|g'_{\Phi(j)}(t)\|_1 \|g^{*}_{h_a}(t)\|_1}, \frac{h_{\Phi(2)} v_1(0)}{\|g'_{\Phi(2)}(t)\|_1}\right), \quad \forall j > 2 \end{aligned} \tag{24}$$

Thus, condition (11) can be replaced with condition (20). ■

IV. Linear Platoon With Benchmark CACC Design

A. Mixed Traffic Platoon Setup

For the CACC controllers, the benchmark structural diagram is shown in Fig. 2, which is a typical design used in PF communication scenario. For the ACC controller, the structure is similar except the absence of the feedforward path $F_i(s)$.

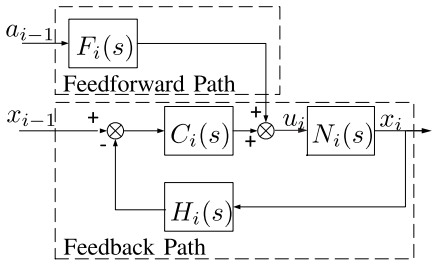

Fig. 2. Linear feedback feedforward controller.

For the car dynamics, the transfer function is adopted as $N_i(s) = \frac{X_i(s)}{U_i(s)} = \frac{1}{(1+\tau_i s)s^2}$ where τ_i is the lumped lag of the i^{th} car's longitudinal dynamics. A proportional derivative (PD) controller is adopted as a cascade controller

$$C_i(s) = K_{p,i} + K_{d,i} s. \tag{25}$$

$K_{p,i} = \omega_i$ and $K_{d,i} = \omega_i^2$ are chosen based on [12] where ω_i is the bandwidth of the system with $\omega_i < \frac{1}{\tau_i}$. Since the CTH spacing policy is adopted, $H_i(s) = h_{\Phi(i)} s + 1$ where $h_\Phi(i)$ is the constant time headway of the i^{th} car with type $\Phi(i)$. For the feedforward controller/filter, we adopt the design from [12]:

$$F_i(s) = \frac{1}{H_i(s) N_i(s) s^2} = \frac{1 + \tau_i s}{1 + h_\Phi(i) s}. \tag{26}$$

Hence, the neighbor motion states transfer function of the CACC and ACC car can be derived as follows, respectively,

$$G^{*}_{\Phi(i)}(s) = \frac{(C_i(s) + s^2 F_i(s)) N_i(s)}{1 + H_i(s) C_i(s) N_i(s)}, \quad \Phi(i) \in C. \tag{27}$$

$$G^{*}_{\Phi(i)}(s) = \frac{C_i(s) N_i(s)}{1 + H_i(s) C_i(s) N_i(s)}, \quad \Phi(i) \in A. \tag{28}$$

For the manual driving car, the well-known Pipe model [24] is adopted: $G^{*}_{\Phi(i)} = \frac{\beta_i e^{-\delta_i s}}{s + \beta_i e^{-\delta_i s}}$, $\Phi(i) \in H$, where β_i is the sensitivity factor and δ_i is the delay of the human driver. Using the Padé approximation $e^{-\delta_i s} \approx \frac{1 - \frac{\delta_i}{2} s}{1 + \frac{\delta_i}{2} s}$ [27], we can get the standard driver model as follows:

$$G^{*}_{\Phi(i)}(s) = \frac{-\delta_i \beta_i s + 2\beta_i}{\delta_i s^2 + (2 - \delta_i \beta_i) s + 2\beta_i}, \ \Phi(i) \in H. \tag{29}$$

B. Platoon Model

We now obtain the state space model for a linear platoon. Let the states of the i^{th} individual car be $\mathbf{x}_i = [x_i, v_i, a_i, u_{ff,i}]^T$ representing the position, velocity, acceleration and feedforward control signal, respectively.

For the leading car, we have $\dot{a}_1 = -\frac{1}{\tau_1} a_1 + \frac{u_r}{\tau_1}$ where u_r is the leading car's reference acceleration profile [18] and its state space form is:

$$\begin{aligned}\dot{\mathbf{x}}_1 &= A_{1,1} \mathbf{x}_1 + B_1 u_r, \\ A_{1,1} &= \begin{pmatrix} 0 & 1 & 0 & 0 \\ 0 & 0 & 1 & 0 \\ 0 & 0 & -\frac{1}{\tau_1} & 0 \\ 0 & 0 & 0 & 0 \end{pmatrix}, \quad B_1 = \begin{pmatrix} 0 \\ 0 \\ \frac{1}{\tau_1} \\ 0 \end{pmatrix}. \end{aligned} \tag{30}$$

For the i^{th} manual driving car ($i \geq 2$), we can convert the transfer function (29) into the following state-space form:

$$\begin{aligned}
\dot{\mathbf{x}}_i &= A_{i,i-1}\mathbf{x}_{i-1} + A_{i,i}\mathbf{x}_i, \ \Phi(i) \in H, \\
A_{i,i-1} &= \begin{pmatrix} 0 & 0 & 0 & 0 \\ 0 & 0 & 0 & 0 \\ 0 & \frac{2\beta_i}{\delta_i} & -\beta_i & 0 \\ 0 & 0 & 0 & 0 \end{pmatrix}, \\
A_{i,i} &= \begin{pmatrix} 0 & 1 & 0 & 0 \\ 0 & 0 & 1 & 0 \\ 0 & -\frac{2\beta_i}{\delta_i} & -\frac{2-\delta_i\beta_i}{\delta_i} & 0 \\ 0 & 0 & 0 & 0 \end{pmatrix}.
\end{aligned} \tag{31}$$

Before giving the state-space representation of the automated following cars ($i \geq 2$) with the control structure in Section IV-A, we define the following:

$$A^*_{i,i} \triangleq \begin{pmatrix} 0 & 1 & 0 & 0 \\ 0 & 0 & 1 & 0 \\ 0 & 0 & -\frac{1}{\tau_i} & 0 \\ 0 & 0 & 0 & -1/h_{\Phi(i)} \end{pmatrix}; \quad T_i \triangleq [0, 0, 1/\tau_i, 0]^T;$$

$$K_{r,i} \triangleq [-K_{p,i}, -K_{d,i} - K_{p,i}h_{\Phi(i)}, -K_{d,i}h_{\Phi(i)}, 1];$$

$$K_{f,i} \triangleq [K_{p,i}, K_{d,i}, 0, 0]; \quad R_i \triangleq [0, 0, 0, 1/h_{\Phi(i)}]^T.$$

For the ACC car $i \geq 2$, we have

$$\dot{\mathbf{x}}_i = A_{i,i-1}\mathbf{x}_{i-1} + A_{i,i}\mathbf{x}_i, \ i \geq 2, \ \Phi(i) \in A, \tag{32}$$

where $A_{i,i} = A^*_{i,i} + T_i K_{r,i}$ and $A_{i,i-1} = T_i K_{f,i}$.

For the CACC car, if $i = 2$, $\Phi(2) \in C$,

$$\dot{\mathbf{x}}_2 = A_{2,1}\mathbf{x}_1 + A_{2,2}\mathbf{x}_2 + B_2 u_r, \tag{33}$$

where $A_{2,1} = T_2 K_{f,2} + R_2[0, 0, 1, 0] + \tau_2 R_2 A_{1,1}(3, :)$, where $A_{1,1}$ is from (30). $A_{2,2} = A^*_{2,2} + T_2 K_{r,2}$, $B_2 = [0, 0, 0, \frac{\tau_2}{\tau_1 h_{\Phi(2)}}]$. If $i > 2$, $\Phi(i) \in C$,

$$\begin{aligned}
\dot{\mathbf{x}}_i &= A_{i,1}\mathbf{x}_1 + A_{i,2}\mathbf{x}_2 + \ldots + A_{i,i}\mathbf{x}_i \\
A_{i,i} &= A^*_{i,i} + T_i K_{r,i}, \\
A_{i,i-1} &= T_i K_{f,i} + R_i[0, 0, 1, 0] + \tau_i R_i A_{i-1,i-1}(3, :), \\
A_{i,i-2} &= \tau_i R_i A_{i-1,i-2}(3, :), \\
&\vdots \\
A_{i,1} &= \tau_i R_i A_{i-1,1}(3, :).
\end{aligned} \tag{34}$$

As a result, the state space model for a mixed traffic platoon with an arbitrary car sequence is as follows:

$$\begin{pmatrix} \dot{\mathbf{x}}_1 \\ \dot{\mathbf{x}}_2 \\ \dot{\mathbf{x}}_3 \\ \vdots \\ \dot{\mathbf{x}}_n \end{pmatrix} = \begin{pmatrix} A_{1,1} & 0 & 0 & \cdots & 0 \\ A_{2,1} & A_{2,2} & 0 & \cdots & 0 \\ A_{3,1} & A_{3,2} & A_{3,3} & \cdots & 0 \\ \vdots & \vdots & \vdots & \ddots & \vdots \\ A_{n,1} & A_{n,2} & A_{n,3} & \cdots & A_{n,n} \end{pmatrix} \begin{pmatrix} \mathbf{x}_1 \\ \mathbf{x}_2 \\ \mathbf{x}_3 \\ \vdots \\ \mathbf{x}_n \end{pmatrix} + \begin{pmatrix} B_1 \\ B_2 \\ 0 \\ \vdots \\ 0 \end{pmatrix} u_r \tag{35}$$

Depending on the car type, the submatrices $A_{i,j}$ and B_i have different formulations as shown above. For example, $A_{i,j}, \ j \leq i-2$ is a zero matrix if i is an ACC or manual car and B_2 is a zero matrix if the 2nd car is not a CACC car. The discrete time model used in Section V is obtained using the zero order hold (ZOH) method [28] for (35).

Theorem 2: Given a mixed traffic platoon according to Definition 1, mixed traffic string stability can be guaranteed by adjusting the time headway of CACC cars or inserting an additional CACC car between the string unstable car and the leading car under the controller structure shown in Fig. 2.

Proof: The proof is based on the verification of all conditions (9)-(11) given in Theorem 1. If there exists a car $\iota > 1$ such that $\|G^{\Lambda}_{\iota,1}(s)\|_{H_\infty} > \|G^*_{h_a}(s)\|_{H_\infty} > 1$ or $\|g^{\Lambda}_{\iota,1}(t)\|_1 > \|g^*_{h_a}(t)\|_1 > 1$, it obviously cannot satisfy the mixed traffic string stability. We will prove that under the proposed control structure shown in Fig. 2, the mixed traffic string stability can be satisfied again by either (a) enlarging time headway of the front CACC car, or (b) inserting an additional CACC car.

(a) Enlarging Time Headway of CACC Cars

By adopting the feedforward filter (26), the transfer function of a CACC car (27) can be rewritten as $G^*_{\Phi(i)}(s) = \frac{1}{H_i(s)} = \frac{1}{h_{\Phi(i)}s+1}$, $\Phi(i) \in C, i > 1$.

Firstly, we show the new motion state transfer function from the leading car to the string unstable car ι satisfies condition (9) via enlarging the time headway of the front CACC car. We start by increasing the time headway of an arbitrary chosen CACC car (car j, $1 < j \leq \iota$, j can be equal to ι if $\Phi(\iota) \in C$) from $h_{\Phi(j)}$ to h^1. Correspondingly, the motion state transfer function from the leading car to car ι becomes $G^{(1),\Lambda}_{\iota,1}(s) = \frac{h_{\Phi(j)}s+1}{h^1 s+1} G^{\Lambda}_{\iota,1}(s)$. We know from the sub-multiplicative property [14] that

$$\left\| \frac{h_{\Phi(j)}s+1}{h^1 s+1} G^{\Lambda}_{\iota,1}(s) \right\|_{H_\infty} \leq \left\| \frac{h_{\Phi(j)}s+1}{h^1 s+1} \right\|_{H_\infty} \left\| G^{\Lambda}_{\iota,1}(s) \right\|_{H_\infty} \tag{36}$$

The equality holds when both H_∞ norms on the right hand side are achieved at the same frequency. It is easy to show that $\underset{s}{\text{argmax}} \left| \frac{h_{\Phi(j)}s+1}{h^1 s+1} \right| = 0$. We also have $\|G^{\Lambda}_{\iota,1}(s)\|_{H_\infty} > 1$ and $\left| G^{\Lambda}_{\iota,1}(s) \right|_{s=0} = 1$, which suggests that the H_∞ norm is achieved at $s \neq 0$. Hence, only the inequality holds.

We can keep increasing the time-headway of the chosen CACC car from h^1 to $h^2 \ldots$ to h^n to h^* with $h^* > h^n > h^{n-1} \ldots > h^2 > h^1$. It is easy to get that, for $\forall \gamma = 1, \ldots, n$, $\underset{s}{\text{argmax}} \left| \frac{h^{\gamma-1}s+1}{h^{\gamma}s+1} \right| = 0$ and

$$\begin{aligned}
&\left\| \frac{h^{\gamma-2}s+1}{h^{\gamma-1}s+1} \cdots \frac{h^1 s+1}{h^2 s+1} \frac{h_{\Phi(j)}s+1}{h^1 s+1} G^{\Lambda}_{\iota,1}(s) \right\|_{H_\infty} > 1, \\
&\left| \frac{h^{\gamma-2}s+1}{h^{\gamma-1}s+1} \cdots \frac{h^1 s+1}{h^2 s+1} \frac{h_{\Phi(j)}s+1}{h^1 s+1} G^{\Lambda}_{\iota,1}(s) \right|_{s=0} = 1,
\end{aligned} \tag{37}$$

which suggests that the H_∞ norm is achieved at $s \neq 0$. Following similar proof as above, we can derive the following:

$$\begin{aligned}
\left\|G_{\iota,1}^{(2),\Lambda}(s)\right\|_{H_\infty} &= \left\|\frac{h^1 s+1}{h^2 s+1} G_{\iota,1}^{(1),\Lambda}(s)\right\|_{H_\infty} \\
&< \left\|\frac{h^1 s+1}{h^2 s+1}\right\|_{H_\infty} \left\|G_{\iota,1}^{(1),\Lambda}(s)\right\|_{H_\infty} \\
&= \left\|G_{\iota,1}^{(1),\Lambda}(s)\right\|_{H_\infty}, \\
\left\|G_{\iota,1}^{(3),\Lambda}(s)\right\|_{H_\infty} &= \left\|\frac{h^2 s+1}{h^3 s+1} G_{\iota,1}^{(2),\Lambda}(s)\right\|_{H_\infty} \\
&< \left\|\frac{h^2 s+1}{h^3 s+1}\right\|_{H_\infty} \left\|G_{\iota,1}^{(2),\Lambda}(s)\right\|_{H_\infty} \\
&= \left\|G_{\iota,1}^{(2),\Lambda}(s)\right\|_{H_\infty}, \\
&\vdots \\
\left\|G_{\iota,1}^{(n),\Lambda}(s)\right\|_{H_\infty} &< \left\|G_{\iota,1}^{(n-1),\Lambda}(s)\right\|_{H_\infty}, \\
\left\|G_{\iota,1}^{(*),\Lambda}(s)\right\|_{H_\infty} &< \left\|G_{\iota,1}^{(n),\Lambda}(s)\right\|_{H_\infty}.
\end{aligned}$$

As we keep increasing the time headway of the chosen CACC car j, the H_∞ norm of motion states transfer function from the leading car to car ι will decrease until it is less than 1 when condition (37) no longer holds, and hence less than $\|G_{h_a}^*(s)\|_{H_\infty}$. This proves the satisfaction of condition (9).

Secondly, we show that the new motion state transfer function satisfies condition (10) via enlarging the time headway of the front CACC car. Similarly, we start by increasing the time headway of the chosen CACC car from $h_{\Phi(j)}$ to h^1. Correspondingly, the motion state transfer function from the leading car to car ι becomes $G_{\iota,1}^{(1),\Lambda}(s) = \frac{h_{\Phi(j)}s+1}{h^1 s+1} G_{\iota,1}^{\Lambda}(s)$. From the Young's Inequality [26], we have

$$\begin{aligned}
&\left\|\mathcal{L}^{-1}\left(\frac{h_{\Phi(j)}s+1}{h^1 s+1} G_{\iota,1}^{\Lambda}(s)\right)\right\|_1 \\
&\qquad \leq \left\|\mathcal{L}^{-1}\left(\frac{h_{\Phi(j)}s+1}{h^1 s+1}\right)\right\|_1 \left\|g_{\iota,1}^{\Lambda}(t)\right\|_1
\end{aligned}$$

The equality holds only when both inversed Laplace tranforms on the right hand side do not change the sign with respect to t [26]. Based on [13], for a transfer function $G(s)$ and its inverse Laplace transform $g(t)$, if $\|g(t)\|_1 > 1$ and $|G(0)| = 1$, $g(t)$ will change the sign. It is easy to show that $|G_{\iota,1}^{(1),\Lambda}(0)| = 1$ by substituting $s = 0$ into the transfer functions (27)-(29). In addition, $\|g_{\iota,1}^{(1),\Lambda}(t)\|_1 > 1$ is also obvious as car ι is string unstable. Therefore, only the inequality holds.

Similarly, we can keep increasing the time-headway of the chosen CACC car from h^1 to $h^2 \ldots$ to h^n to h^* with $h^* > h^n > h^{n-1} \ldots > h^2 > h^1$. It is then easy to get that for $\forall \gamma = 1, \ldots, n$, the following (in)equalities hold:

$$\begin{aligned}
&\left|\frac{h^{\gamma-2}s+1}{h^{\gamma-1}s+1} \cdots \frac{h^1 s+1}{h^2 s+1} \frac{h_{\Phi(j)}s+1}{h^1 s+1} G_{\iota,1}^{\Lambda}(s)\right|_{s=0} = 1, \\
&\left\|\mathcal{L}^{-1}\left(\frac{h^{\gamma-2}s+1}{h^{\gamma-1}s+1} \cdots \frac{h^1 s+1}{h^2 s+1} \frac{h_{\Phi(j)}s+1}{h^1 s+1} G_{\iota,1}^{\Lambda}(s)\right)\right\|_1 > 1,
\end{aligned} \tag{38}$$

which suggests that $\mathcal{L}^{-1}\left(\frac{h^{\gamma-1}s+1}{h^{\gamma}s+1} \ldots \frac{h^1 s+1}{h^2 s+1} \frac{h_{\Phi(j)}s+1}{h^1 s+1} G_{\iota,1}^{\Lambda}(s)\right)$ will change sign. Therefore, following the same proof, the following inequalities hold:

$$\begin{aligned}
\|g_{\iota,1}^{(2),\Lambda}(t)\|_1 &= \left\|\mathcal{L}^{-1}\left(\frac{h^1 s+1}{h^2 s+1}\right) * g_{\iota,1}^{(1),\Lambda}(t)\right\|_1 \\
&< \left\|\mathcal{L}^{-1}\left(\frac{h^1 s+1}{h^2 s+1}\right)\right\|_1 \left\|g_{\iota,1}^{(1),\Lambda}(t)\right\|_1 = \left\|g_{\iota,1}^{(1),\Lambda}(t)\right\|_1, \\
\|g_{\iota,1}^{(3),\Lambda}(t)\|_1 &= \left\|\mathcal{L}^{-1}\left(\frac{h^2 s+1}{h^3 s+1}\right) * g_{\iota,1}^{(2),\Lambda}(t)\right\|_1 \\
&< \left\|\mathcal{L}^{-1}\left(\frac{h^2 s+1}{h^3 s+1}\right)\right\|_1 \left\|g_{\iota,1}^{(2),\Lambda}(t)\right\|_1 = \left\|g_{\iota,1}^{(2),\Lambda}(t)\right\|_1, \\
&\vdots \\
\|g_{\iota,1}^{(n),\Lambda}(t)\|_1 &< \|g_{\iota,1}^{(n-1),\Lambda}(t)\|_1, \\
\|g_{\iota,1}^{(*),\Lambda}(t)\|_1 &< \|g_{\iota,1}^{(n),\Lambda}(t)\|_1.
\end{aligned}$$

As we keep increasing the time headway of the CACC car, the 1-norm of the inverse Laplace transform of motion states transfer function from the leading car to car ι will decrease until it is less than or equal to 1 when condition (37) no longer holds, and hence less than $\|g_{h_a}^*(t)\|_1$. Therefore, condition (10) is satisfied.

For condition (11), there exists an exact value of the right hand side of the inequality for a specific platoon. This means we can always find a flexible range for the leading car's velocity profile to satisfy the velocity fluctuation constraint. As a result, condition (11) is also satisfied.

(b) *Inserting an Additional CACC Car*

We now show that the string stability can also be satisfied by inserting a CACC car in front of the string unstable car ι. Here, the time headway of the inserted CACC car is chosen as h^* which is equal to the larger time headway used in Part (a). Since the platoon size is increased by 1, the motion state transfer function from the leading car to the $\iota+1^{\text{th}}$ car becomes $G_{\iota+1,1}^{\Lambda}(s) = \frac{1}{h^* s+1} G_{\iota,1}^{\Lambda}(s) = \frac{1}{h_{\Phi(j)}s+1} G_{\iota,1}^{(*),\Lambda}(s)$, where $h_{\Phi(j)}$ is the time headway of the arbitrarily chosen CACC car in Part (a). The string stability using $G_{\iota,1}^{(*),\Lambda}(s)$ has been proved in Part (a). It is also easy to show that $\|\frac{1}{h_{\Phi(j)}s+1}\|_{H_\infty} = 1$ and $\|\mathcal{L}^{-1}(\frac{1}{h_{\Phi(j)}s+1})\|_1 = 1$. From the sub-multiplication and Young's inequality, we have $\|G_{\iota+1,1}^{\Lambda}(s)\|_{H_\infty} \leq \|\frac{1}{h_{\Phi(j)}s+1}\|_{H_\infty} \|G_{\iota,1}^{(*),\Lambda}(s)\|_{H_\infty} \leq \|G_{\iota,1}^{(*),\Lambda}(s)\|_{H_\infty} \leq \|G_{h_a}^*(s)\|_{H_\infty}$ and $\|g_{\iota+1,1}^{\Lambda}(t)\|_1 \leq \|\mathcal{L}^{-1}(\frac{1}{h_{\Phi(j)}s+1})\|_1 \|g_{\iota,1}^{(*),\Lambda}(t)\|_1 \leq \|g_{\iota,1}^{(*),\Lambda}(t)\|_1 \leq \|g_{h_a}^*(t)\|_1$. Hence, conditions (9) and (10) are satisfied. For condition (11), the proof is same as Part (a). This completes the proof. ■

V. Human-Centered CACC Controller Design

In this section, an MPC-like blending ratio control algorithm is proposed to trade off among physical comfort, psychological comfort, fuel economy as well as the traffic throughput under the guarantee of mixed traffic string stability.

The V2V communication allows the introduction of the feedforward controller, which decreases the time headway of the CACC car to 0.7 seconds without breaking the H_∞

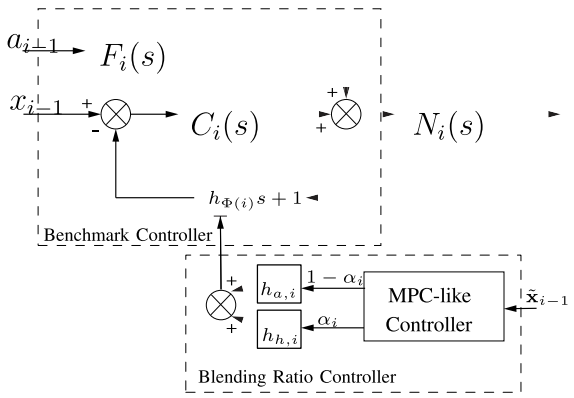

Fig. 3. The proposed MPC-like blending ratio controller.

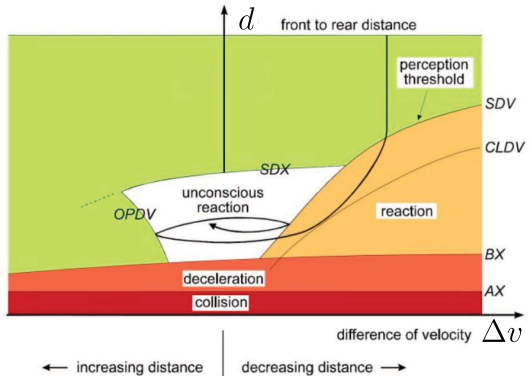

Fig. 4. The AP car-following model [36].

string stability in the real test scenario [29]. As a result, the traffic throughput will be improved significantly. On the other hand, the recommended time headway for a manual driver is 1.4-1.8 seconds [30], [31], which is much larger than that of the CACC system. Comparatively, the shorter time-headway can make the system more sensitive to the change of the preceding car's velocity change, which can be reflected by the car jerk. The above factors can make the human driver feel uncomfortable when riding with the CACC system. Under this circumstance, more brakes may be applied, which in turn deteriorates fuel economy and falls in exactly the opposite direction of the CACC's design goal. Based on these reasons, although the shorter time-headway of the current CACC controller design can improve traffic throughput, in practice, driver comfort and fuel economy can be deteriorated. To facilitate the adoption of CACC systems, it is therefore necessary to design a human-centered CACC controller that can make a good balance between traffic throughput and driving experience.

In this paper, we seek to address this issue by finding an optimal time headway $h_{d,i}$ of the feedback controller in the automated cars, which blends costs among the driver comfort, traffic throughput and fuel-economy. The variable time headway is selected as the optimal solution to an MPC-like blending ratio controller. In [32], a similar controller is used to find the optimal blending ratio between the human control input and the automatic system control signal for the motion control of a mobile robot. This is an MPC-like optimization but not exactly MPC such as the work in [33]. For the CACC/ACC controller design considered here, an optimal blending ratio α_i between the human preferred time-headway $h_{h,i}$ and CACC/ACC performance oriented time-headway $h_{a,i}$ is computed as follows:

$$h_{\Phi(i)} = \alpha_i h_{h,i} + (1-\alpha_i)h_{a,i}, \quad \Phi(i) \in A \cup C. \tag{39}$$

The human preferred time headway is considered from the comfort aspects, which can also be regarded as the upper bound of the optimal variable time headway. In contrast, the CACC/ACC performance oriented time-headway mainly considers the traffic throughput, which can be regarded as the lower bound of the optimal time-headway. The basic structure of our human-centered CACC controller is shown in Fig. 3.

In our MPC-like controller, the optimal blending ratio will be found for each control horizon T when the cost function is minimized in the predication horizon T_b. We formulate the cost function as the weighted sum of traffic throughput, fuel economy (in terms of control input), and comfort (both physical and psychological) for each CACC car i as:

$$J_i = c_1 \sum^{T_b} \|d_i\|_2 + c_2 \sum^{T_b} \|u_i\|_2 + c_3 \sum^{T_b} \|jerk_i\|_2 + c_4 \sum^{T_b} \|z_i\|. \tag{40}$$

where c_1, c_2, c_3 and c_4 are the corresponding coefficients. The term d_i is the inter-distance between the i^{th} and $(i-1)^{\text{th}}$ car as defined in Section II. A smaller inter-distance indicates a higher traffic throughput. The control input (i.e. desired acceleration u_i) is introduced to optimize fuel economy. Firstly, the fuel consumption of a car is dominated by car acceleration if the engine operates in normal areas [34]. The suppression of the desired acceleration level will help to reduce fuel consumption. A lot of existing optimization algorithms [17], [19] have shown good fuel economy improvements by punishing the desired acceleration. Secondly, although there are more accurate models to show the fuel consumption [35], these models are determined by the type of the car. Since we seek to show the general optimal algorithm, it is not reasonable to pick one specific model over others. The term $jerk_i$ is the longitudinal jerk of the i^{th} car, $jerk_i = \dot{a}_i$, which can be obtained directly from the discretized state space model discussed in Section IV-B. The jerk can reflect physical comfort of the driver and driving smoothness. The fourth part z_i is explained as follows. Fig. 4 shows the driving regimes in terms of inter-distance and inter-velcoity for the psychophysical car-following model (i.e. AP model) proposed in [22]. In this model, different driving regimes are separated based on the human driver's perceptual thresholds (i.e. SDX, OPDV, SDV and BX). BX represents the minimum following threshold for the human driver. SDV is the perceptual threshold for the human driver to detect approaching of the preceding car. OPDV is the perceptual threshold for driver to realize leaving of the preceding car. If the above changes are detected by the human driver, i.e. the inter-vehicle states exceed the thresholds, corresponding acceleration/deceleration will be generated until the car goes into the unconscious regime. In the unconscious regime, a human driver cannot perceive any

relative motion with the preceding car despite generating small acceleration/deceleration unconsciously. If the CACC cars can stay more within the unconscious regime, the human driver will have fewer chances to perceive the velocity change of the preceding car. For one thing, human will have smoother driving experience without feeling anxious about the rapid interaction with the preceding car. For another, the human workload in monitoring the CACC car operation can be reduced, since human's nerve is less stimulated during the normal operating mode. Because one of the objectives of the CACC cars is to enhance driving comfort as well as reducing workload, our human-centered CACC controller will utilize the above human perception property to improve the riding experience.

To encourage the CACC car to stay more within the unconscious reaction regime, the punishment factor z_i is added to the cost function J_i for every time step in the predication horizon when the driver is out of the unconscious regime, i.e.

$$z_i = \begin{cases} \text{constant}, & \text{if outside of unconscious regime} \\ 0, & \text{if inside unconscious regime.} \end{cases}$$

Moreover, constraints have been added to the MPC-like controller to guarantee the mixed traffic string stability defined in Definition 2. As a result, we have the following constrains (41)-(44) for the i^{th} CACC car in the optimization of (40). Firstly, we give the motion fluctuation constraints of the CACC cars. Here, the constraints are with respect to two consecutive cars, which are more conservative than the mixed traffic string stability definition but can leave more flexibility to the constraints on the manual driving cars.

$$\begin{aligned} &\|\lambda_i(t) - \lambda_i(0)\|_p \le \|\lambda_{i-1}(t) - \lambda_{i-1}(0)\|_p, \\ &\forall i > 1, t > 0, \Phi(i) \in A \cup C, p \in \{2, \infty\}. \end{aligned} \tag{41}$$

The following constraints of the manual driving cars' motion states are also added to the MPC-like controller of the i^{th} CACC car considering that the manual driving car cannot be manipulated directly:

$$\|\lambda_{i+j}(t) - \lambda_{i+j}(0)\|_2 \le \|G^*_{h_a}(s)\|_\infty \|\lambda_1(t) - \lambda_1(0)\|_2, \tag{42}$$

$$\begin{aligned} &\|\lambda_{i+j}(t) - \lambda_{i+j}(0)\|_\infty \le \|g^*_{h_a}(t)\|_1 \|\lambda_1(t) - \lambda_1(0)\|_\infty, \\ &\forall z \ge j \ge 0, \quad t > 0, \ \Phi(i), \ \Phi(i+z+1) \in A \cup C, \\ &\{\Phi(i+1), \quad \Phi(i+2) \dots \Phi(i+z)\} \in H. \end{aligned} \tag{43}$$

We also use the time to collision (TTC) to formulate the safety constraint [19]. A minimum distance $d_{\min}$ is also set to avoid an unacceptably short inter-distance.

$$\begin{aligned} &d_{i+j}(t) \ge \max\{TTC\left(v_{i+j}(t) - v_{i+j-1}(t)\right), d_{\min}\}, \\ &\forall z \ge j \ge 0, \ t > 0, \Phi(i), \quad \Phi(i+z+1) \in A \cup C, \\ &\{\Phi(i+1), \quad \Phi(i+2) \dots \Phi(i+z)\} \in H. \end{aligned} \tag{44}$$

Furthermore, the predicted preceding car's motion states $\tilde{\mathbf{x}}_i$ is necessary to generate the outputs of the i^{th} car's dynamics in the prediction horizon. For a CACC car, if its preceding car is also a CACC car, the preceding car's motion states can be directly received from V2V communication. However, if its preceding car is a manual driving car, the motion states are not available. The automated car can have communication with the most immediate automated preceding car directly or indirectly through relay communication.

When the immediate preceding car has no communication capability, i.e. a manual driving or ACC car, its motion states can be predicted based on the predicted motion states of the most immediate preceding CACC car and the driving models of the cars without communication capacity. In addition, the performance of the predictor depends on the accuracy of the driving models adopted. Here, for the sake of illustration and simplicity, perfect driving models are used in the predictor. In our future works, the design of a driving model estimator and predictor will be investigated.

Nevertheless, the MPC-like controller might be infeasible when constraints (41)-(44) cannot be satisfied. Therefore, the constraint soften method [19] has been adopted. For the string stability constraints (41)-(43), we have the following changes:

$$\begin{aligned} &\frac{\|\lambda_i(t) - \lambda_i(0)\|_p}{\|\lambda_{i-1}(t) - \lambda_{i-1}(0)\|_p} \le 1 + \epsilon\gamma_s, \\ &\forall i > 1, \quad t > 0, \ \Phi(i) \in A \cup C, \ p \in \{2, \infty\}, \end{aligned} \tag{45}$$

$$\frac{\|\lambda_{i+j}(t) - \lambda_{i+j}(0)\|_2}{\|G^*_{h_a}(s)\|_\infty \|\lambda_1(t) - \lambda_1(0)\|_2} \le 1 + \epsilon\gamma_s, \tag{46}$$

$$\frac{\|\lambda_{i+j}(t) - \lambda_{i+j}(0)\|_\infty}{\|g^*_{h_a}(t)\|_1 \|\lambda_1(t) - \lambda_1(0)\|_\infty} \le 1 + \epsilon\gamma_s, \tag{47}$$

$$\begin{aligned} &\forall z \ge j \ge 0, \ t > 0, \ \Phi(i), \Phi(i+z+1) \in A \cup C, \\ &\{\Phi(i+1), \ \Phi(i+2) \dots \Phi(i+z)\} \in H. \end{aligned}$$

where γ_s is the relaxation of the upper bounds 1 given in (41)-(43), and ϵ is called the slack variable. Moreover, the constraint soften method is not applicable in safety constraint (44) considering it is not reasonable to soften the minimum inter-distance. Since our algorithm is to find the optimal time headway blending ratio, the safety distance constraint is hard to break as long as the low level controller $C_i(s)$ has prompt response. If the extreme scenario happens, the safety-oriented deceleration should override autonomous cruise control. Correspondingly, the augmented cost function (40) becomes:

$$\begin{aligned} J_i = c_1 \sum^{T_b} \|d_i\|_2 + c_2 \sum^{T_b} \|u_i\|_2 + c_3 \sum^{T_b} \|jerk_i\|_2 \\ + c_4 \sum^{T_b} \|z_i\| + \rho\epsilon^2. \end{aligned} \tag{48}$$

where ρ is the weighting ratio. The overall human-centered CACC control algorithm is shown in Algorithm 1.

VI. Simulation Results

A. Mixed Traffic String Stability in Linear Platoon

In this section, a 7-car mixed traffic platoon as shown in Fig. 5 is simulated. The leading car is an automated car under an autonomous controller. It can broadcast information to the following car. The 2nd car, 3rd car and 5th cars are CACC cars, which can communicate with their immediate

Algorithm 1 MPC-Like Blending Ratio Controller

INPUT:
$h_{h,i}$: Human preferred time headway
OUTPUT:
$h_{d,i}$: Optimal time headway for each time step
for each time horizon T_b **do**
$\tilde{\mathbf{x}}_{i-1} \leftarrow$ Get the motion states of the immediate preceding car from the motion predictor
$x_0 \leftarrow$ Update the initial states
  for α_i= 0 to 1 **do**
 $h_{d,i} \leftarrow \alpha_i h_{h,i} + (1-\alpha_i) h_{a,i}$
 $x_i, \lambda_i \leftarrow$ Update states based on the discretized model in Section IV-B
 $d_i, u_i, Jerk_i, z_i \leftarrow$ Calculate the inter-distance, control input, jerk, and consciousness punishment factor
CONSTRAINTS: (41),(43),(43),(44)
    if no α_i can satisfy the constraints **then**
      $\epsilon \leftarrow$ Calculate the slack variable from soften constraints (45),(46),(47)
      $J_i \leftarrow$ Calculate the cost function from (48)
    else
      $J_i \leftarrow$ Calculate the cost function from (40)
    end if
  end for
$\alpha_i \leftarrow \text{argmin} J_i$
$h_{\Phi(i)} \leftarrow$ Update the time headway from (39)
end for

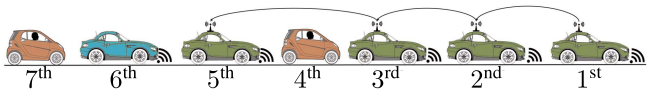

Fig. 5. A 7-car mixed traffic platoon.

preceding CACC car. Since there is no direct communication with its preceding manual driving car, the 5th car degrades to ACC despite it may still have communication with the 3rd car. The 4th car and 7th car are manual driving cars. In addition, the 6th car is an ACC car without communication capability.

We assume that each CACC, ACC, or manual driving car in the platoon has identical dynamics with the same parameters. This means that the neighbor motion states transfer function of the 2nd car is the same as the 3rd car, i.e. $G^*_{\Phi(2)}(s) = G^*_{\Phi(3)}(s)$. For the ACC cars, we have $G^*_{\Phi(5)}(s) = G^*_{\Phi(6)}(s)$. All the manual driving cars are modeled by the standard Pipe model with $\beta = 0.368$ and $\delta = 1.55$ [24], i.e. $G^*_{\Phi(4)} = G^*_{\Phi(7)} = G^*_{h_a}(s)$. All these cars adopt the dynamic structure shown in Section IV-A. The detailed parameters values are shown in Table I. The time headway of CACC ($h_{CACC} > 0.7s$ in practice) and ACC ($h_{ACC} > 1s$) are within the reasonable ranges [13], [29]. The controller gain satisfies the bandwidth requirement $\omega < 1/\tau$ [12]. The value of τ is also used in [19].

In this section, we will check the mixed traffic string stability of the linear mixed platoon under the controller structure in Section IV. We can obtain the H_∞ norm of the neighbor motion state transfer function and the 1 norm of its inverse Laplace transform for every car:

TABLE I
SIMULATION PARAMETERS

Parameters	Values	Parameters	Values
τ_{CACC}	0.2	τ_{ACC}	0.2
h_{CACC}	0.8	h_{ACC}	1.3
ω_{CACC}	0.7	ω_{ACC}	2.0
β	0.368	δ	1.55

$$\begin{aligned}
\|G^*_{\Phi(2)}\|_{H_\infty} &= \|G^*_{\Phi(3)}\|_{H_\infty} = 1,\ \Phi(2) = \Phi(3) \in C.\\
\|G^*_{\Phi(5)}\|_{H_\infty} &= \|G^*_{\Phi(6)}\|_{H_\infty} = 1,\ \Phi(5) = \Phi(6) \in A.\\
\|G^*_{\Phi(4)}\|_{H_\infty} &= \|G^*_{\Phi(7)}\|_{H_\infty} = 1.03,\ \Phi(4) = \Phi(7) \in H.\\
\|g^*_{\Phi(2)}\|_1 &= \|g^*_{\Phi(3)}\|_1 = 1,\ \Phi(2) = \Phi(3) \in C.\\
\|g^*_{\Phi(5)}\|_1 &= \|g^*_{\Phi(6)}\|_1 = 1,\ \Phi(5) = \Phi(6) \in A.\\
\|g^*_{\Phi(4)}\|_1 &= \|g^*_{\Phi(7)}\|_1 = 1.328,\ \Phi(4) = \Phi(7) \in H.
\end{aligned}$$

As seen from the above calculation, the ACC and CACC cars in the platoon satisfy the condition in Proposition 1. Hence, we only need to check the motion state transfer function from the leading car to 4th and 7th manual driving cars:

$$\begin{aligned}
\|G^{\Lambda}_{4,1}(s)\|_{H_\infty} &= 1 \le \|G^*_{h_a}(s)\|_{H_\infty} = 1.03.\\
\|G^{\Lambda}_{7,1}(s)\|_{H_\infty} &\le \|G^{\Lambda}_{4,1}(s)\|_{H_\infty}\|G^{\Lambda}_{7,4}(s)\|_{H_\infty} = 1\times 1\\
&\le \|G^*_{h_a}(s)\|_{H_\infty} = 1.03.\\
\|g^{\Lambda}_{4,1}(s)\|_1 &= 1.152 \le \|g^*_{h_a}(s)\|_{H_\infty} = 1.328.\\
\|g^{\Lambda}_{7,1}(s)\|_1 &\le \|g^{\Lambda}_{4,1}(s)\|_1\|g^{\Lambda}_{7,4}(s)\|_1 = 1.259\\
&\le \|g^*_{h_a}(s)\|_1 = 1.328.
\end{aligned}$$

The above inequalities show that conditions (18) and (19) are satisfied. For condition (20), we have the following inequality:

$$\begin{aligned}
&\|v_1(t) - v_1(0)\|_\infty\\
&\quad \le \min\left(\frac{h_{\Phi(i)} v_1(0)}{\|g'_{\Phi(i)}(t)\|_1 \|g^*_{h_a}(t)\|_1}\right),\quad i = \{2,4,5\},
\end{aligned}$$

where cars 2, 4 and 5 represent three types of cars considered in this simulation. It is easy to show that the above inequality holds for same type of cars in the platoon. Here, we adopt the human perferred time headway proposed in [31], i.e. $h_{\Phi(4)} = h_{\Phi(7)} = 1.4s$. By calculating the corresponding 1 norm of the above inequality, we have $\|v_1(t) - v_1(0)\|_\infty < \min\{0.753, 0.753, 0.337\} v_1(0)$. That is, $0.663 v_1(0) < v_1(t) < 1.337 v_1(0)$ (33.7% variation). This inequality gives us the boundary of the leading car's speed profile, which is a wide enough range for the highway condition. Here, the conservative human time headway $h_a = 1.4s$ is adopted. The human preferred time-headway can also be much larger, e.g., the well adopted 1.8s [30], and the corresponding allowed variance becomes 44.7%.

A set of simulation corresponding to the specific leading car's velocity profile is then generated. As shown in Fig. 6, the maximal velocity fluctuation is $(20 - 14.37)/20 = 0.28 < 0.337$. Hence, the safety of the platoon can

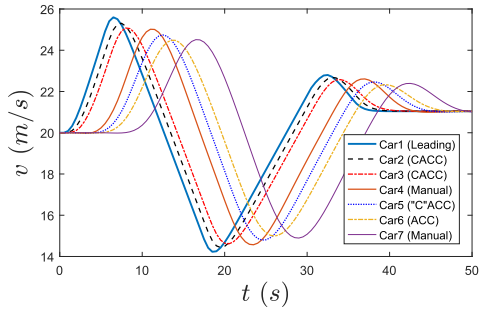

Fig. 6. Linear platoon velocity response.

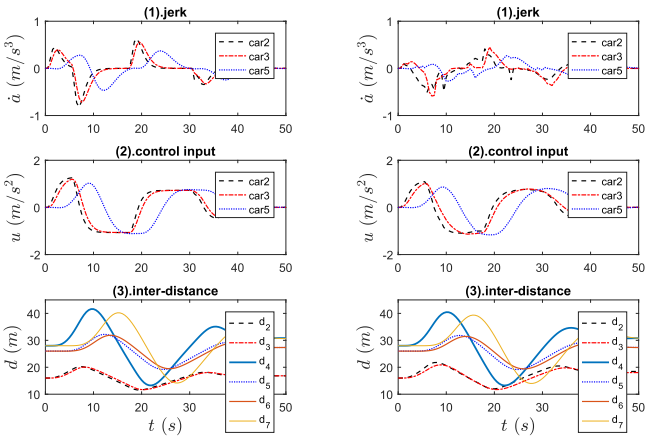

(a) (b)

Fig. 7. Response comparison. (a) Benchmark response. (b) MPC-like controller response.

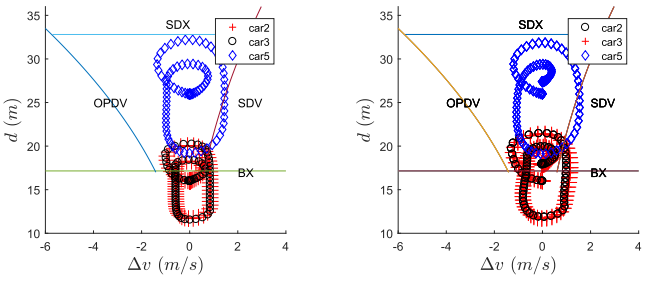

(a) (b)

Fig. 8. Unconscious regime distribution. (a) Benchmark design distribution. (b) MPC-like controller distribution.

be guaranteed. The safety criterion can also be checked and confirmed from Fig. 7a(3). The jerk and control input are also shown in this figure. As can be seen, the general behavior is acceptable with guarantee of mixed traffic string stability. From Fig. 8a, the 2nd and 3rd CACC cars rarely stay within the unconscious regime.

B. Mixed Traffic With Human-Centered CACC Design

In this section, human-centered CACC designs are applied to the 2nd, 3rd and 5th CACC cars to find the optimal time headway for their conventional controllers based on the trade-offs among the driver's physical comfort, psychological comfort, control input and traffic throughput. Note that although there is no feedfoward path for the 5th car, the MPC-like controller can still find an optimal time headway for the feedback loop. Since the 2nd and 3rd car have the same feedback and feedforward controller structure, they share the same MPC-like parameters. Since the 5th car only has the feedback loop with a larger time headway, it will have another set of MPC-like parameters. The main parameters are given in Table II. With $T = 0.5$ and $T_b = 2.5$, the 7-car simulation can be finished within 2 mins using a laptop with a Core i7 processor.

TABLE II
OPTIMAL CONTROLLER PARAMETERS

Para_CACC	Values	Para_ACC	Values
$\{T, T_b\}$	{0.5,2.5}	$\{T, T_b\}$	{0.5,2.5}
$\{c_1, c_2, c_3, c_4\}$	{75,150,4,70}	$\{c_1, c_2, c_3, c_4\}$	{50,70,4,70}
$\{\rho, \gamma_s\}$	{50,0.01}	$\{\rho, \gamma_s\}$	{50,0.01}
$\{h_h, h_a\}$	{1.4,0.8}	$\{h_h, h_a\}$	{1.4,1.3}

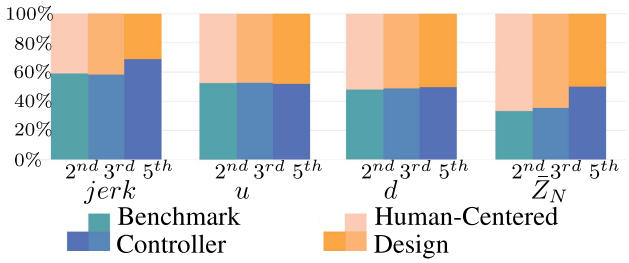

Fig. 9. Comparison of *jerk*, u, d, and $\bar{Z}_N$ for the 2nd, 3rd and 5th cars under the benchmark and the human-centered controllers.

With the detailed controller design mentioned in Section V, we generate a simulation under the same scenario as that in Section VI-A however introducing the MPC-like controllers in the 2nd, 3rd and 5th cars. The results are shown in Figs. 7b and 8b. As can be seen from the figures, the jerk decreases largely under the MPC-like controller, which can improve the drivers' physical comfort. The CACC cars also have more occurrences within the unconscious regime that can contribute to the drivers' psychological comfort. Under the benchmark and MPC-like control, we calculate the 2 norm of jerk, control input, and inter-distance for the CACC cars, i.e. the 2nd, 3rd, and 5th cars, respectively. We also count the time steps that these cars stay within the unconscious regime ($\bar{Z}_N$). After normalization between the benchmark and human-centered controllers, the statistical comparisons are shown in Fig. 9. As a result, both the physical and psychological comfort are largely improved using the human-centered CACC design. There are also small improvements in the fuel economy (in terms of control input) while the traffic throughput (in terms of inter-distance) sacrifices a little. Although the improvement in fuel economy is relatively small, the increase (6%) is still acceptable as a minor factor in the multi-objective optimization. The increase of inter-distance is also reasonable since the benchmark controller is performance-oriented.

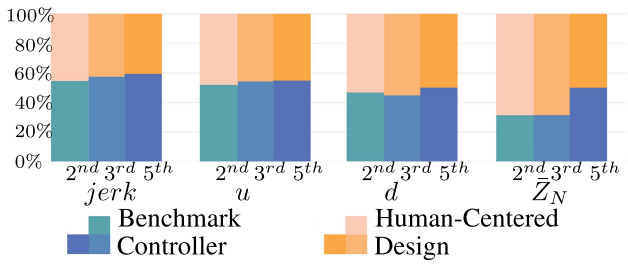

Fig. 10. Comparison between the benchmark and the human-centered controllers with more complicated dynamics (0.1s delay and 0.3s lag).

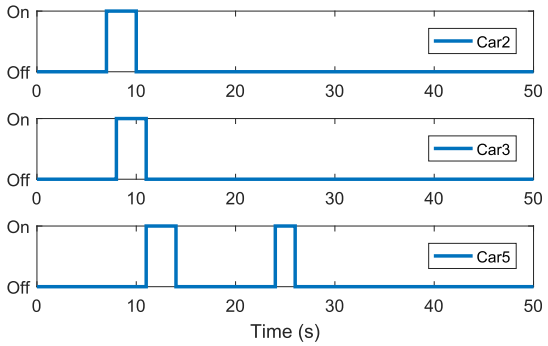

Fig. 11. Application of soften constraints in the more complicated dynamics (0.1s delay and 0.3s lag).

To further verify the performance of the MPC-like blending ratio controller, a 0.1s actuator delay and a larger lag term 0.3s have been added into the vehicle longitudinal dynamics in Section IV-A. The simulation is generated with the same leading car speed profile as shown in Fig. 6. The statistical comparison is shown in Fig. 10. The proposed blending ratio controller still largely improves the physical and psychological comfort despite greater sacrifice of the inter-distance performance. In addition, soften constraints of the automated cars have been activated because of the complexity of the vehicle dynamics as shown in Fig.11.

VII. Conclusion and Future Research

In this paper, a novel mixed traffic string stability definition is proposed, in which both motion state fluctuation and safety guarantees are considered. A mixed traffic string stability theorem and the relaxed proposition are proposed based on the novel criteria. Under the benchmark controller design, mixed traffic string stability is proved analytically. This provides guidance on the traffic sequence management and automated controller design in mixed traffic scenarios. The mixed traffic string stability can also be applied to analyze the platoon behavior under other nonlinear or linear controllers in general. The impact of communication topologies on the collective behavior of platoons is a very critical problem, which poses new challenges in CACC controller design. In our future research, we will extend the theorem to other common communication typologies, such as the bidirectional (BD) topology and predecessor-following leader (PFL) topology [2].

Moreover, a human-centered controller is proposed to optimize the driver's physical comfort, psychological comfort, fuel economy, and traffic throughput. In this paper, the unconscious regime in the AP model is used to quantify the psychological comfort of a human driver. From the simulation, the human-centered controller improves both physical and psychological comfort of the drivers. For the unconscious regime of the AP model, we directly use the time headway value from the literature, which can be revised through the calibration based on real driving data. Moreover, the predictor in our human-centered design is assumed to be perfect, which may lose fidelity in real world scenarios. In our future works, the human-centered controller will be combined with the model predictor. The MPC-like algorithm can also be used as a framework for future research since it does not put any constraint on the type of feedback and feedforward controller.

References

[1] L. Xiao and F. Gao, "A comprehensive review of the development of adaptive cruise control systems," *Veh. Syst. Dyn.*, vol. 48, no. 10, pp. 1167–1192, 2010.

[2] S. E. Li, Y. Zheng, K. Li, and J. Wang, "An overview of vehicular platoon control under the four-component framework," in *Proc. IEEE Intell. Veh. Symp. (IV)*, Jun. 2015, pp. 286–291.

[3] K. C. Dey *et al.*, "A review of communication, driver characteristics, and controls aspects of cooperative adaptive cruise control (CACC)," *IEEE Trans. Intell. Transp. Syst.*, vol. 17, no. 2, pp. 491–509, Feb. 2016.

[4] D. Swaroop and J. K. Hedrick, "String stability of interconnected systems," *IEEE Trans. Autom. Control*, vol. 41, no. 3, pp. 349–357, Mar. 1996.

[5] H. Hao and P. Barooah, "On achieving size-independent stability margin of vehicular lattice formations with distributed control," *IEEE Trans. Autom. Control*, vol. 57, no. 10, pp. 2688–2694, Oct. 2012.

[6] P. Seiler, A. Pant, and K. Hedrick, "Disturbance propagation in vehicle strings," *IEEE Trans. Autom. Control*, vol. 49, no. 10, pp. 1835–1842, Oct. 2004.

[7] J. K. Hedrick and D. Swaroop, "Dynamic coupling in vehicles under automatic control," *Veh. Syst. Dyn.*, vol. 23, pp. 209–220, Jan. 1994.

[8] C.-Y. Liang and H. Peng, "Optimal adaptive cruise control with guaranteed string stability," *Veh. Syst. Dyn., Int. J. Veh. Mech. Mobility*, vol. 32, nos. 4–5, pp. 313–330, 1999.

[9] S. Sheikholeslam and C. A. Desoer, "Longitudinal control of a platoon of vehicles with no communication of lead vehicle information: A system level study," *IEEE Trans. Veh. Technol.*, vol. 42, no. 4, pp. 546–554, Nov. 1993.

[10] R. Toscano, *Structured Controllers for Uncertain Systems*. London, U.K.: Springer-Verlag, 2013.

[11] C.-Y. Liang and H. Peng, "String stability analysis of adaptive cruise controlled vehicles," *JSME Int. J. Ser. C Mech. Syst., Mach. Elements Manuf.*, vol. 43, no. 3, pp. 671–677, 2000.

[12] G. J. L. Naus, R. P. A. Vugts, J. Ploeg, M. J. G. van de Molengraft, and M. Steinbuch, "String-stable CACC design and experimental validation: A frequency-domain approach," *IEEE Trans. Veh. Technol.*, vol. 59, no. 9, pp. 4268–4279, Nov. 2010.

[13] A. Bose and P. A. Ioannou, "Analysis of traffic flow with mixed manual and semiautomated vehicles," *IEEE Trans. Intell. Transp. Syst.*, vol. 4, no. 4, pp. 173–188, Dec. 2003.

[14] J. Ploeg, N. van de Wouw, and H. Nijmeijer, "L_p string stability of cascaded systems: Application to vehicle platooning," *IEEE Trans. Control Syst. Technol.*, vol. 22, no. 2, pp. 786–793, Mar. 2014.

[15] *Preliminary Statement of Policy Concerning Automated Vehicles*, Nat. Highway Safety Admin. (NHTSA), Washington, DC, USA 2013, pp. 1–14.

[16] E. Weiss, "Bodily and mental pain," *Int. J. Psycho-Anal.*, vol. 15, p. 1, Jan. 1934.

[17] S. Li *et al.*, "MPC based vehicular following control considering both fuel economy and tracking capability," in *Proc. IEEE Veh. Power Propuls. Conf. (VPPC)*, Sep. 2008, pp. 1–6.

[18] X. Wang and Y. Wang, "Human-aware autonomous control for cooperative adaptive cruise control (CACC) systems," in *Proc. ASME Dyn. Syst. Control Conf.*, 2015, p. V002T31A001.

[19] S. Li, K. Li, R. Rajamani, and J. Wang, "Model predictive multi-objective vehicular adaptive cruise control," *IEEE Trans. Control Syst. Technol.*, vol. 19, no. 3, pp. 556–566, May 2011.

[20] L.-H. Luo, H. Liu, P. Li, and H. Wang, "Model predictive control for adaptive cruise control with multi-objectives: Comfort, fuel-economy, safety and car-following," *J. Zhejiang Univ. Sci. A*, vol. 11, no. 3, pp. 191–201, 2010.
[21] S. Jones, "Cooperative adaptive cruise control: Human factors analysis," U.S. Dept. Transport., Federal Highway Admin., Res., Develop., Technol., McLean, VA, USA, Tech. Rep. FHWA-HRT-13-045, Oct. 2013.
[22] R. Wiedemann and U. Reiter, "Microscopic traffic simulation: The simulation system mission, background and actual state," CEC Project ICARUS, Brussels, Belgium, Final Rep. V1052, 1992, vol. 2.
[23] T. Nagatani, "Traffic jams induced by fluctuation of a leading car," *Phys. Rev. E, Stat. Phys. Plasmas Fluids Relat. Interdiscip. Top.*, vol. 61, no. 4, p. 3534, 2000.
[24] R. E. Chandler, R. Herman, and E. W. Montroll, "Traffic dynamics: Stxudies in car following," *Oper. Res.*, vol. 6, no. 2, pp. 165–184, 1958.
[25] D. Helbing and B. A. Huberman, "Coherent moving states in highway traffic," *Nature*, vol. 396, no. 6713, pp. 738–740, 1998.
[26] H. Koch, D. Tataru, and M. Visan, *Dispersive Equations and Nonlinear Waves*, vol. 45. Basel, Switzerland: Birkhäuser, 2014.
[27] G. A. Baker, Jr., and P. Graves-Morris, *Padé Approximants* (Encyclopedia of Mathematics and Its Applications), vol. 59. Cambridge, U.K.: Cambridge Univ. Press, 1996.
[28] K. C. Pohlmann, *Principles of Digital Audio*. Oxford, U.K.: Butterworth-Heinemann, 1985.
[29] J. Ploeg, B. T. Scheepers, E. van Nunen, N. van de Wouw, and H. Nijmeijer, "Design and experimental evaluation of cooperative adaptive cruise control," in *Proc. 14th Int. IEEE Conf. Intell. Transp. Syst. (ITSC)*, Oct. 2011, pp. 260–265.
[30] Highway Capacity Manual, "Special report 209," 3rd ed., Transp. Res. Board, Washington, DC, USA, Tech. Rep., 1985, p. 985, vol. 1.
[31] H. Ota, "Distance headway behavior between vehicles from the viewpoint of proxemics," *IATSS Res.*, vol. 18, no. 2, pp. 5–14, 1994.
[32] J. G. Storms and D. M. Tilbury, "Blending of human and obstacle avoidance control for a high speed mobile robot," in *Proc. Amer. Control Conf.*, 2014, pp. 3488–3493.
[33] Y. Zheng, S. E. Li, K. Li, F. Borrelli, and J. K. Hedrick, "Distributed model predictive control for heterogeneous vehicle platoons under unidirectional topologies," *IEEE Trans. Control Syst. Technol*, vol. 25, no. 3, pp. 899–910, May 2017.
[34] J. Zhang and P. A. Ioannou, "Longitudinal control of heavy trucks in mixed traffic: Environmental and fuel economy considerations," *IEEE Trans. Intell. Transp. Syst.*, vol. 7, no. 1, pp. 92–104, Mar. 2006.
[35] J. Heywood, *Internal Combustion Engine Fundamentals*. New York, NY, USA: McGraw-Hill, 1988.
[36] *VISSIM 5.10 User Manual*, PTV AG, Karlsruhe, Germany, 2008.

Fangjian Li (S'16) received the B.S. degree in vehicle engineering from the Hefei University of Technology, Hefei, China, in 2014, and the M.S. degree in automotive engineering from Clemson University, Clemson, SC, USA, in 2016, where he is currently pursuing the Ph.D. degree with the Department of Mechanical Engineering. His research interests include controls and human-centered design in intelligent transportation systems.

Yue Wang (S'06–M'11–SM'16) received the B.S. degree from Shanghai University, China, in 2005, and the M.S. and Ph.D. degrees from the Worcester Polytechnic Institute in 2008 and 2011, respectively. She held a post-doctoral position with the Electrical Engineering Department, University of Notre Dame. In 2012, she joined Clemson University, where she is currently the Warren H. Owen–Duke Energy Assistant Professor of engineering. Her research interests include cooperative control and decision-making for human–robot collaboration systems, cyber-physical systems, and multi-agent systems. She was a recipient of the Air Force Young Investigator Award in 2016 and the NSF CAREER Award in 2015. She is the Chair of the IEEE CSS TC on Manufacturing Automation and Robotic Control and a member of the IEEE RAS TC on Multi-Robot Systems.